Affinity maturation of a broadly neutralizing human monoclonal antibody that prevents hepatitis C virus infection

Zhen-Yong Keck[1], Yong Wang[1], Patrick Lau[1], Garry Lund[2], Sneha Rangarajan[3,4], Catherine Fauvelle[5,6], Grant C. Liao[7], Frederick W. Holtsberg[7], Kelly L. Warfield[7], M. Javad Aman[7], Brian G. Pierce[3], Thomas R. Fuerst[3], Justin R. Bailey[8], Thomas F. Baumert[5,6,9] Roy A. Mariuzza[3,4], Norman M. Kneteman[10,11] and Steven K. H. Foung[1#]

Supplementary Methods

Construction, characterization, and expression of various HC84.26 yeast display libraries introducing mutations. (A) For light chain shuffle library: The light chain repertoire was derived from peripheral blood B lymphocytes that were obtained from an asymptomatic individual infected with HCV genotype 2b infection. The library was constructed in the pYD2 vector, designated as pYD2.HC84-VK/VL, as previously described (1). The VH fragment of the pYD2.HC84.26 was amplified by primer extension with forward primer GAP5 (5'-TTA AGC TTC TGC AGG CTA GTG-3') and reverse primer HuJHR: (5'-ACC TCC GGA GCC ACC TCC GCC TGA ACC GCC TCC ACC TGT CGA CCC TGA-3'). The HC84.26 light chain shuffle library was created by ligating amplified VH fragments (10 µg) to pre-digested pYD2.HC84-VK/VL (NcoI/SalI, 50 µg) in Saccharomyces cerevisiae strain EBY100 through gap repairing. Library characterization and induction has been described previously (1). (B) For random mutagenesis library: Creation of random mutagenesis single-chain Fv fragment (scFv) yeast display library was carried out as previously described (2). Briefly, the gene encoding the wt HC84.26 scFv was randomized using a Stratagene GeneMorph® II random mutagenesis kit to obtain a low to high mutagenesis rate. The resulting repertoire (10 µg) was cloned into pYD2 vector in Saccharomyces cerevisiae strain EBY100 through gap repair. Library was cultured and induced after characterization of the library. (C) For site-directed mutagenesis scFv yeast display libraries: To further increase the binding affinity and/or to increase breadth of neutralization, amino acid change was sequentially introduced in VH-CDR1/CDR2 using a QuikChange II site-directed mutagenesis kit with degenerated primers (NNS) as described (2). Library construction and growth was carried out as described above. (D) Isolation of candidate clones: MACS and FACS sorting of antigen-specific affinity-improved scFv clones and cloning of immunoglobulin genes were carried out using previously described protocol (2).

Protein expression and purification. The HC84.26.5D antibody was expressed as a scFv by *in vitro* folding from inclusion bodies produced in *Escherichia coli*. The scFv construct consisted of the

heavy chain variable (V_H) region (residues Glu1–Ser127) connected to the light chain variable (V_L) region (residues Gln1–Leu110) by an 18-residue linker (GSTGGGGSGGGGSGGGGS). The HC84.26.5D scFv was cloned into the expression vector pET-26b (Novagen) and expressed as inclusion bodies in BL21(DE3) *E. coli* cells (Novagen). Bacteria were grown at 37 ^{o}C in LB medium to an absorbance of 0.6–0.8 at 600 nm, and induced with 1 mM isopropyl-β-D-thiogalactoside. After incubation for 3 h, the bacteria were harvested by centrifugation and resuspended in 50 mM Tris-HCl (pH 8.0) containing 0.1 M NaCl and 2 mM EDTA; cells were disrupted by sonication. Inclusion bodies were washed extensively with 50 mM Tris-HCl (pH 8.0) and 2% (v/v) Triton X-100, then dissolved in 8 M urea, 50 mM Tris-HCl (pH 8.0), and 10 mM DTT. For *in vitro* folding, inclusion bodies were diluted into ice-cold folding buffer containing 1 M L-arginine-HCl, 50 mM Tris-HCl (pH 8.0), 1 mM EDTA, 3 mM reduced glutathione, and 0.9 mM oxidized glutathione, to a final protein concentration of 60 mg/l. After 72 h at 4 °C, the folding mixture was concentrated 50-fold, dialyzed against 50 mM MES (pH 6.0), and centrifuged to remove aggregates. Correctly folded HC84.26.5D scFv was then purified using sequential Superdex 75 HR and MonoQ columns (GE Healthcare).

Crystallization and data collection. For crystallization of the HC84.26.5D–$E2_{434–446}$ complex, HC84.26.5D (10 mg/ml) was mixed with $E2_{434–446}$ peptide (NTGWLAGLFYQHK) (GenScript) in a 1:5 molar ratio. Crystals were grown at room temperature in sitting drops containing 1 μl of the complex solution mixed with 1 μl of reservoir solution consisting of 1.6 M sodium phosphate monobasic, 0.4 M potassium phosphate dibasic, and 0.1 M sodium phosphate dibasic/citric acid (pH 4.2). For data collection, crystals were soaked briefly in a cryoprotectant containing mother liquor plus 20% (v/v) 2-methyl-2,4-pentanediol before flash freezing in liquid nitrogen. X-ray diffraction data for the HC84.26.5D–$E2_{434–446}$ complex were collected at beamline X29A of the Brookhaven National Synchrotron Light Source Laboratory. The HC84.26.5D–$E2_{434–446}$ crystal belongs to space group $P2_12_12_1$ with one molecule per asymmetric unit. Diffraction data were processed using Mosflm (3). Scaling and reduction were performed with programs from the CCP4 suite (4). The data set is 97% complete to 2.0 Å resolution with R_{merge} = 0.145. Data collection statistics are shown in Supplementary Table 2.

Structure determination and refinement. The structure of the HC84.26.5D–$E2_{434–446}$ complex was solved by molecular replacement with Phenix.MRage (5) using ensemble search models for the V_H and V_L domains of the HC84.26.5D scFv. These ensembles were chosen based on sequence homology to the corresponding V_H (Protein Data Bank accession codes: 4JZO, 4HJO, 3QOT, 4DN3) and V_L

(4AIX, 4AJO, 4QHK, 4DAG) chains. A difference electron density map was calculated to reveal the $E2_{434–446}$ peptide and model building of the peptide was based exclusively on the visible electron density. The model was refined to an R_{work} of 0.22 (R_{free} = 0.26) using iterative cycles of model building in Coot (6) and refinement using Phenix (7). Refinement statistics are summarized in Supplementary Table 2. Stereochemical parameters were evaluated with PROCHECK (8).

Protein Data Bank accession code. Coordinates and structure factors for the HC84.26.5D–$E2_{434–446}$ complex have been deposited in the Protein Data Bank under accession code 4Z0X.

Computational mutagenesis. Prior to *in silico* mutagenesis, we briefly minimized the HC84.26.5D–$E2_{434–446}$ crystal structure using the constrained relax protocol of Rosetta version 3.5 (9) to alleviate any minor structural defects that would potentially bias modeling results. We then used Rosetta 2.0 (10) to perform structural modeling of point mutants, followed by scoring of mutant structures using ZAFFI 1.1 (11). ZAFFI 1.1 scores were converted to $\Delta\Delta G$s using the previously determined linear regression from a dataset of 24 experimentally measured T cell receptor point mutants (11).

Modeling of the HC84.26.5D–E2 core complex. To generate a model of HC84.26.5D with E2 core, we superposed the HC84.26.5D–$E2_{434–446}$ complex onto the E2 core structure (12) via root-mean-square fitting of the backbone atoms of the core epitope helix (residues 437–443) from both crystal structures. We used Modeller (13) to model residues linking the epitope termini to E2 core. Due to a clash between the fitted antibody and the non-epitope region of E2 core (primarily between the V_H of HC84.26.5D and the N-terminus of the E2 core structure), we used Rosetta's Floppytail protocol (14) to generate 2400 minimized models of the HC84.26.5D complex with E2, via flexible backbone modeling of E2 residues 429–452, while keeping the epitope region rigid and fixed to the bound antibody using pairwise distance constraints. Residues 429–452 were selected for flexible modeling as this region is bounded at either end by disulfide bonds, but is on the surface of E2 core and thought to adopt multiple conformations based on structural data (15). The top model from the set of 2400 was selected based on ZRANK2 score (16).

Supplementary References

1. Keck ZY, Xia J, Wang Y, Wang W, Krey T, Prentoe J, Carlsen T, Li AY, Patel AH, Lemon SM, et al. Human monoclonal antibodies to a novel cluster of conformational epitopes on HCV E2 with resistance to neutralization escape in a genotype 2a isolate. *PLoS Pathog.* 2012;8(4):e1002653

2. Wang Y, Keck ZY, Saha A, Xia J, Conrad F, Lou J, Eckart M, Marks JD, and Foung SK. Affinity maturation to improve human monoclonal antibody neutralization potency and breadth against hepatitis C virus. *J Biol Chem.* 2011;286(51):44218-33
3. Leslie AGW, Powell HR. Processing diffraction data with Mosflm. *Evolving Methods for Macromolecular Crystallography.* 2007;245: 41-51.
4. Winn MD, et al. Overview of the CCP4 suite and current developments. *Acta Crystallogr D Biol Crystallogr.* 2011;67:235-242.
5. Bunkóczi G, Echols N, McCoy AJ, Oeffner RD, Adams PD, Read RJ. Phaser.MRage: automated molecular replacement. *Acta Crystallogr D Biol Crystallogr.* 2013;69:2276-2286.
6. Emsley P, Lohkamp B, Scott WG, Cowtan K. Features and development of Coot. *Acta Crystallogr D Biol Crystallogr.* 2011;66:486-501.
7. Adams PD, et al. PHENIX: a comprehensive Python-based system for macromolecular structure solution. *Acta Crystallogr D Biol Crystallogr.* 2010;66:213-221.
8. Laskowski RA, MacArthur MW, Moss DS, Thornton JM. PROCHECK: a program to check the stereo chemical quality of protein structures. *J Appl Crystallogr.* 1993;26:283-291.
9. Leaver-Fay A, Tyka M, Lewis SM, Lange OF, Thompson J, Jacak R, Kaufman K, Renfrew PD, Smith CA, Sheffler W, et al. ROSETTA3: an object-oriented software suite for the simulation and design of macromolecules. *Methods Enzymol.* 2011;487(545-74.
10. Kortemme T, and Baker D. A simple physical model for binding energy hot spots in protein-protein complexes. *Proc Natl Acad Sci U S A.* 2002;99(22):14116-21.
11. Pierce BG, Hellman LM, Hossain M, Singh NK, Vander Kooi CW, Weng Z, Baker BM. Computational design of the affinity and specificity of a therapeutic T cell receptor. *PLoS Comput Biol.* 2014;10(2):e1003478.
12. Kong L, et al. Hepatitis C virus E2 envelope glycoprotein core structure. *Science.* 2013; 342:1090-1094.
13. Webb B, Sali A. Protein structure modeling with MODELLER. *Methods in Molecular Biology.* 2014;1137**:**1-15.
14. Kleiger G, Saha A, Lewis S, Kuhlman B, Deshaies RJ. Rapid E2-E3 assembly and disassembly enable processive ubiquitylation of cullin-RING ubiquitin ligase substrates. *Cell.* 2009;139:957-968.
15. Deng L, et al. Discrete conformations of epitope II on the hepatitis C virus E2 protein for antibody-mediated neutralization and nonneutralization. *Proc Natl Acad Sci USA.* 2014;111:10690-10695.
16. Pierce B, Weng Z. A combination of rescoring and refinement significantly improves protein docking performance. *Proteins.* 2008;72:270-279.

Supplementary Table 1A. Mutations identified in HCV 1b E2 glycoprotein in control mice (B.A862 and B.A869) and in HC84.26.5D treated mouse with breakthrough infection (B.A818)

Amino Acid Position HCV 1b	Mouse			
	Inoculum	Breakthrough	Control 1	Control 2
N384	D (1/10)*			D (1/10)
Y386	H (1/10)			
T388	A (1/10)			
G389		W (1/10)		
R394	K (1/10)			
N395				D (1/10)
L399	F (1/10)			
N415		S (1/10)		
N417			D (1/10)	
T435		A (1/10)		
I438	T (1/10)			
S450		F (1/10)		
M456			D (1/10)	
A457				G (1/10)
I462		T (1/10)		
T473	S (1/10)			
S480		P (1/10)		P (1/10)
Q492	R (2/10)			
V497				A (1/10)
V502	A (1/10)			
S512	G (1/10)			
V515		A (1/10)		
F522	S (4/10)		S (4/10)	S (3/10)
V524	A (1/10)			
N532				Y (1/10)
L539			P (1/10)	
N548				I (1/10)
M555				T (2/10)
N570				D (1/10)
V574	A (1/10)		A (1/10)	
T580	I (1/10)			
P590				S (1/10)
E591			D (1/10)	
A595	T (1/10)			G (1/10)
F624				S (1/10)
I626			T (1/10)	
K628				R (1/10)
M631			T (1/10)	
V636			A (1/10)	
R648				G (1/10)

**Ten individual clones were sequenced per mouse serum.*

Supplemental Table 1B. Mutations identified in HCV 1b E1 glycoprotein in control mice (B.A862 and B.A869) and in HC84.26.5D treated mouse with breakthrough infection (B.A818)

Amino Acid Position	Mouse			
HCV 1b	Inoculum	Breakthrough	Control 1	Control 2
Y192		C (2/10)*		
E193	G (1/10)			
V197	A (1/10)			
D218				G (1/10)
M219				T (1/10)
S252		N (1/10)		
V253		A (1/10)		A (1/10)
M275			T (1/10)	
Q289				R (1/10)
H316		Q (1/10)		
M324			T (1/10)	
T329	A (1/10)			P (1/10)
A331			G (2/10)	
I332		V (1/10)		
D346				G (1/10)
N367	S (1/10)			
V381	G (1/10)/A(1/10)			

**10 individual clones were sequenced per mouse serum*

Supplementary Table 2. Data collection and structure refinement statistics

	HC84.26.5D–E2$_{434–446}$
Data collection	
Resolution (Å)[a]	41.9–2.00 (2.07–2.00)
Space group	$P2_12_12_1$
Unit cell (Å)	a = 50.44, b = 50.78, c = 69.36
Unique reflections	15,410
Completeness (%)[a]	99.02 (94.3)
R_{merge}	0.145
Mean $I/\sigma(I)$[a]	14.8 (3.5)
Refinement	
R_{work} (%)[b]	22.5
R_{free} (%)[b]	27.0
RMSDs from ideality	
Bond length (Å)	0.007
Bond angles (^{o})	1.39
Ramachandran plot statistics (%)	
Favored	94
Forbidden	1.7

[a]Values in parentheses are statistics for the highest resolution shell.
[b]$R_{work} = \Sigma||F_o| - |F_c||/\Sigma|F_o|$, where F_c is the calculated structure factor. R_{free} is as for R_{work} but calculated fora randomly selected 10.0% of reflections not included in the refinement.

Supplementary Table 3. HC84.26.5D–E2$_{434–446}$ interactions

	Peptide	HC84.26.5D
Heavy Chain		
Hydrogen bonds	L441 O	S101 N
Hydrophobic interactions	W437	F55
	L438	M59
	L441	I52
		F55
		M59
		L100
	F442	V33
		I52
		M59

Light Chain		
Hydrogen bonds	Y443 O	S93 N
	K446 Nζ	G28 O
		K30 O
		D50 Oδ2
Hydrophobic interactions	F442	W90
	Y443	W90
	Q444	Y31
Ionic interactions	K446 Nζ	D50 Oδ1
Aromatic stacking interactions	Y443	W90

Contact residues were identified by measuring distances between atoms using the CONTACT program in CCP4 (2). Cut-off distances of 3.4 and 4.0 Å were used for hydrogen bonds and van der Waals contacts, respectively.

Supplementary Table 4. Predicted HC84.26.5D binding affinity change for E2 residue 446 mutants

Mutant	$\Delta\Delta G$, kcal/mol[a]	Fold Change[a]
K446E	1.5	13
K446N	1.5	13
K446A	1.1	6.2

[a]Predicted $\Delta\Delta G$ was calculated using Rosetta (12) and ZAFFI (13), which was then used to determine binding decrease fold change at 25 °C.

Supplemental Figure 1

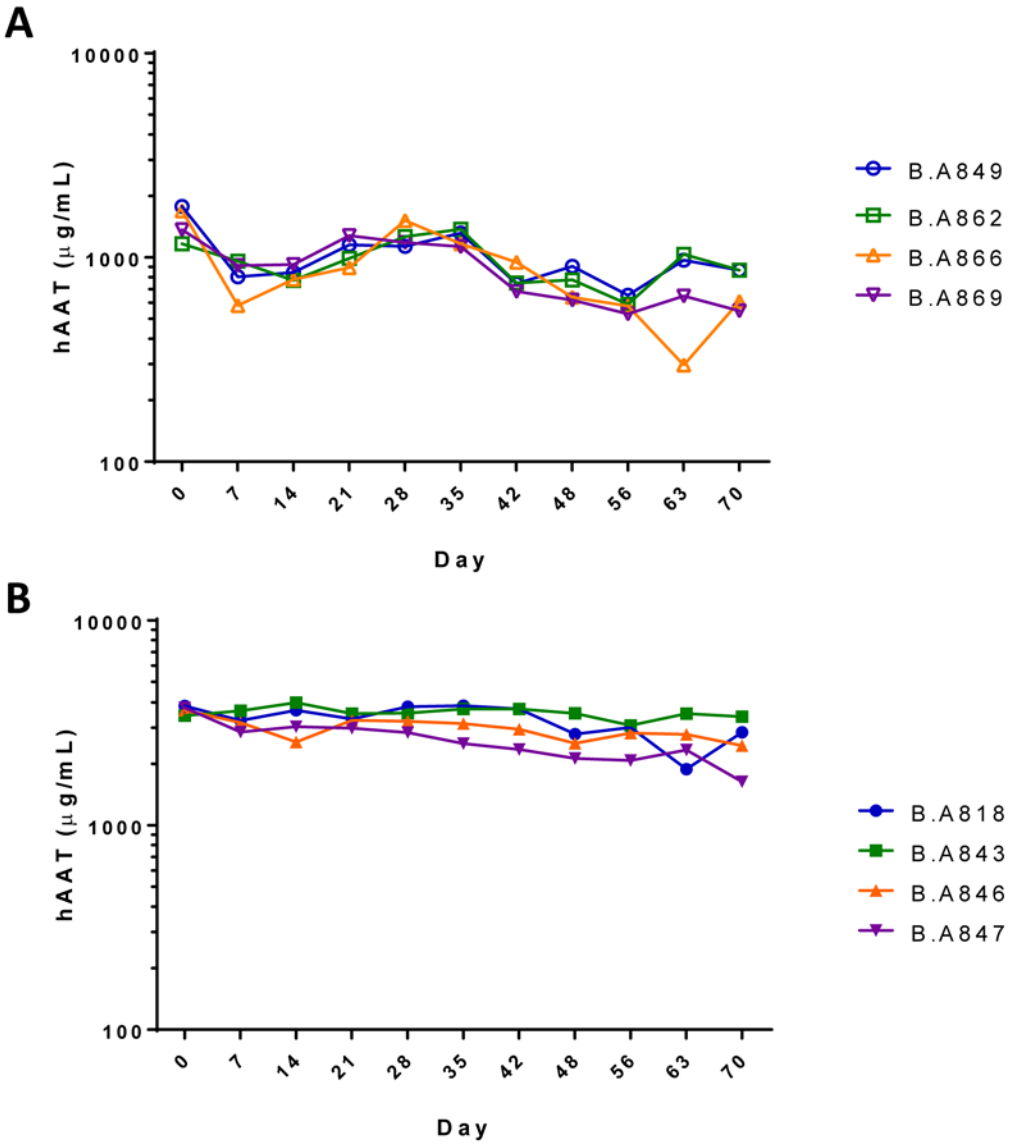

S. Fig. 1: Serum human alpha-1 antitrypsin (hAAT) levels in human liver chimeric alb-uPA/SCID mice treated with (**A**) a control HMAb, R04 and (**B**) HC84.26.5D. Serum hAAT was measured by a sandwich enzyme-linked immunosorbent assay employing a goat anti-hAAT primary capture antibody (#81902, Diasorin) and sheep anti-hAAT secondary antibody conjugated to horseradish peroxidase (#CL20000APHP, Cedarlane Laboratories).

Supplementary Figure 2

A

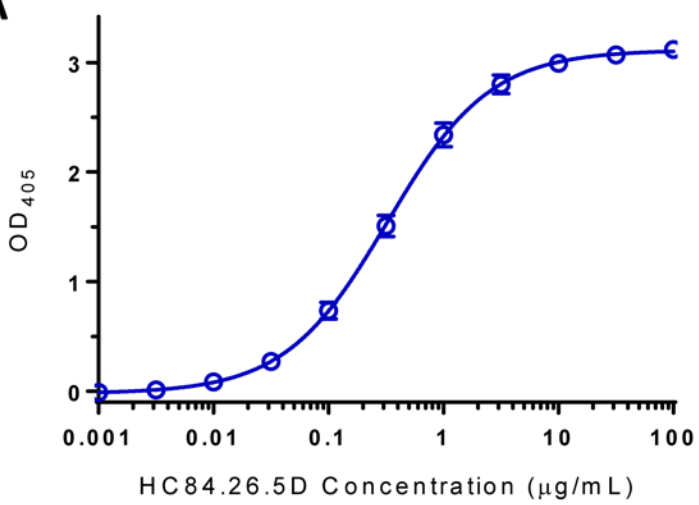

B

Expected (µg/mL)	Calculated (µg/mL)	%AR
1.00	**0.977**	97.7
0.30	**0.257**	85.7
0.10	**0.074**	73.8

S. Fig. 2: (**A**) A standard curve for HC84.26.5D was generated starting at 100 µg/mL and serially diluted in semi-log steps to 0.001 µg/mL. Three separate concentrations of HC84.26.5D were spiked into neat normal mouse serum to generate the quality control samples. (**B**) A 1:100 dilution of each sample was determined in the modified ELISA. The back-calculated concentrations for these samples were within an acceptable range for analytical recovery, indicating naive mouse sera did not have a significant effect on ELISA readout at a 1:100 dilution.